PAPER

Triazole-acetate functionalized gold nanoparticles for colorimetric Pb(II) sensing†

I-Lin Lee, Yi-Ming Sung and Shu-Pao Wu*

New triazole-acetate functionalized gold nanoparticles (TTA–AuNPs) for sensitive and selective colorimetric detection of Pb^{2+} were developed. Aggregation of TTA–AuNPs was induced immediately in the presence of Pb^{2+}, yielding a color change from wine-red to purple. This Pb^{2+}-induced aggregation of TTA–AuNPs was monitored by the bare eye and UV-vis spectroscopy with a detection limit of 16.7 nM. TTA–AuNPs showed excellent selectivity toward Pb^{2+} compared to other metal ions through the interaction between the carboxyl group and triazole structure of TTA and Pb^{2+}. The best detection of Pb^{2+} was achieved in a pH range from 5 to 10. Furthermore, TTA–AuNPs were applied to detect Pb^{2+} in lake water with low interference.
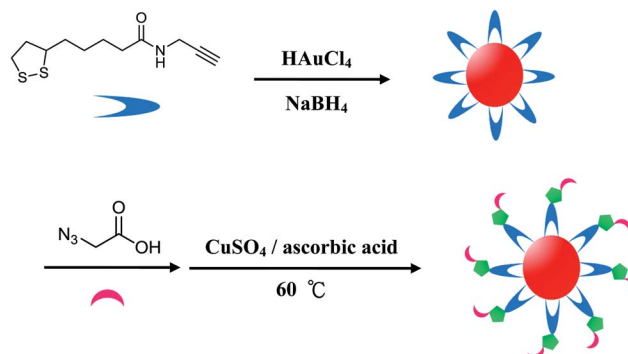
1. Introduction

Lead is one of the most toxic heavy metal elements. Because lead is widely used, such as in gasoline, pipes, paint pigments, and batteries, lead contamination has become a serious environmental problem.[1] Lead can cause damage to the nervous, immune, and cardiovascular systems and induce various health problems, including memory loss, anemia, gout, and hypertension.[2] Owing to the extreme toxicity of lead, the US Environmental Protection Agency (EPA) established the standard maximum concentration level of lead in drinking water to be 15 ppb (15 ng mL^{-1}; 72.4 nM). Therefore, the development of ultrasensitive and quantitative detection of lead is an important issue for environmental protection and disease treatment.

Several analytical methods for the detection of lead ions have been proposed, including atomic absorption spectrometry (AAS),[3] inductively coupled plasma mass spectroscopy (ICP-MS),[4] and electrochemistry.[5,6] However, since these methods require sophisticated instruments, they cannot be easily employed in on-site assays. Colorimetric assays based on functionalized gold nanoparticles (AuNPs) have provided a simple way to overcome these limitations.

AuNPs are highly studied nanomaterials and widely used in a range of applications including: sensing, electronics, and surface enhanced Raman spectroscopy. The surface plasma resonance (SPR) absorption of AuNPs is extremely sensitive to their size, shape, surrounding media, and inter-particle distances.[7,8] Many AuNPs-based colorimetric sensors use the inter-particle plasmon coupling caused by the analyte-induced aggregation of AuNPs to detect analyte.[9] In these assays, analyte-triggered aggregation of AuNPs causes a red shift in the SPR absorption band, resulting in a red-to-blue color change. The distance-dependent SPR absorption of AuNPs has become a useful tool for the development of colorimetric sensing of various analytes, such as metal ions[10–18] and anions.[19–21]

In this report, triazole-acetate functionalized gold nanoparticles (TTA–AuNPs) were synthesized for detecting Pb^{2+}. The gold nanoparticles were prepared through the borohydride-mediated reduction of $HAuCl_4$. 5-(1,2-Dithiolan-3-yl)-*N*-(prop-2-yn-1-yl)pentanamide (TP) was attached to the surface of AuNPs through the dithiol group. Finally, the azide part of azidoacetic acid and the acetylene part of TP were combined to form a triazole structure on the surface of AuNPs through a click reaction. The synthesized 2-(4-((5-(1,2-dithiolan-3-yl)pentanamido)methyl)-1*H*-1,2,3-triazol-1-yl)acetic acid–AuNPs (TTA–AuNPs) can be used for metal ion detection (Scheme 1). Metal ions such as Ag^+, Al^{3+},

Department of Applied Chemistry, National Chiao Tung University, Hsinchu, Taiwan 300, Republic of China. E-mail: spwu@mail.nctu.edu.tw; Fax: +886-3-5723764; Tel: +886-3-5712121 ext. 56506

Scheme 1 Synthesis of TTA–AuNPs.

Ca^{2+}, Cd^{2+}, Co^{2+}, Cu^{2+}, Cr^{3+}, Fe^{2+}, Fe^{3+}, Hg^{2+}, Mg^{2+}, Mn^{2+}, Ni^{2+}, Pb^{2+}, and Zn^{2+} were tested for metal ion selectivity but Pb^{2+} was the only metal ion that caused the aggregation of TTA–AuNPs. This caused the SPR absorption band of the TTA–AuNPs to shift to a longer wavelength, and consequently a color change from wine-red to purple. This color change can be used to detect the presence of Pb^{2+} ions. The SPR absorption at 700 nm directly indicates the degree of TTA–AuNPs aggregation caused by the addition of Pb^{2+} ions.

2. Materials and methods

2.1 Chemicals

Hydrogen tetrachloroaurate(III) tetrahydrate was purchased from Showa. Lipoic acid, N,N-diisopropylethylamine, $AgClO_4 \cdot \chi H_2O$ and $Pb(ClO_4)_2 \cdot 3H_2O$ were purchased from Acros. Propargylamine, O-(benzotriazol-1-yl)-N,N,N',N'-tetramethyluronium hexafluorophosphate (HBTU), bromoacetic acid, sodium ascorbate, $Al(ClO_4)_3 \cdot 9H_2O$, and $Cr(ClO_4)_3 \cdot 6H_2O$ were purchased from Alfa Aesar. Sodium borohydride, sodium azide, copper sulfate, $Ca(ClO_4)_2 \cdot 4H_2O$, $Cd(ClO_4)_2 \cdot \chi H_2O$, $CoCl_2 \cdot 6H_2O$, $Cu(BF_4)_2 \cdot \chi H_2O$, $Fe(BF_4)_2 \cdot 6H_2O$, $FeCl_3 \cdot 6H_2O$, $Hg(ClO_4)_2 \cdot \chi H_2O$, $Mg(ClO_4)_2 \cdot 6H_2O$, $Ni(CH_3CO_2) \cdot 4H_2O$, $Zn(BF_4)_2 \cdot \chi H_2O$ and KBr were purchased from Sigma-Aldrich. $K_2Cr_2O_7$ and $MnSO_4 \cdot H_2O$ were purchased from Riedel-de Haen. For all aqueous solutions, deionized water (resistivity, 18.0 MΩ cm at 25 °C) purified by Millipore Direct-Q water purification unit was used.

2.2 Instruments

Absorption spectra were measured on an Agilent 8453 UV-vis spectrometer (Santa Clara, CA, USA) using a 1.0 cm quartz cell. IR spectra were recorded with KBr pellets on Bomem DA8.3 FTIR spectrometer (Quebec, Canada). HR-TEM images were obtained from JEOL JEM-3000F high-resolution transmission electron microscope (Tokyo, Japan). The average size of nanoparticles was statistically determined by measuring the diameter of 150 particles from the HR-TEM image using ImageJ software. ICP-MS data were acquired on ICP-MS Perkin Elmer, SCIEX ELAN 5000 (Waltham, MA, USA).

2.3 Synthesis of TTA–AuNPs

5-(1,2-Dithiolan-3-yl)-N-(prop-2-yn-1-yl)pentanamide (TP) and azidoacetic acid were synthesized according to the ref. 22 and 23. Gold nanoparticles were prepared by reducing $HAuCl_4$ with sodium borohydride. All glassware was thoroughly cleaned with aqua regia (3 : 1, HCl/HNO_3) and rinsed with deionized water prior to use. Briefly, to 100 mL deionized water, $HAuCl_4$ (80 mM, 270 μL) and TP (10 mM, 50 μL) were added and stirred for 15 min. Freshly prepared sodium borohydride (0.1 M, 1 mL) was added dropwise to the mixture and stirred for 2 h. The color of the aqueous solution became wine-red, indicating that TP-capped gold nanoparticles formed. Then azidoacetic acid (10 mM, 50 μL) was added to the TP–AuNPs solution. The mixture was stirred for 15 min, and heated to 60 °C. To this mixture, a solution of sodium ascorbate (20 mM, 100 μL) mixed with copper sulfate (2 mM, 100 μL) was added slowly and stirred

for a further 2 h. After cooled to room temperature, TTA–AuNPs were purified by dialysis membrane (Spectra/Pro7 Membrane, MWCO 3500) for 3 h, with three changes of the deionized water (at 1 h interval), to remove impurities.

2.4 Colorimetric detection of Pb^{2+} ions

To a 1.0 mL of solution containing TTA–AuNPs, different metal ions (5 μM) were added separately. The mixture were maintained at room temperature for 10 min and then transferred separately into a 1.0 cm quartz cell. The absorption spectra were recorded by UV-vis spectrometer.

2.5 Analysis of lake water samples

A water sample from the lake located in NCTU, Hsinchu, Taiwan, was collected and filtered through a 0.2 μm membrane. To the 500 μL of lake water, different volumes (25, 45, and 75 μL) of Pb^{2+} standard solution (100 μM) were spiked separately. The spiked samples were then added to the 500 μL of TTA–AuNPs solutions and maintained at room temperature for 10 min. The final concentrations of Pb^{2+} were 2.5, 4.5, and 7.5 μM, respectively. The analytical results were obtained by ICP-MS and the developed sensing method.

3. Results and discussion

3.1 Synthesis and characterization of TTA–AuNPs

Gold nanoparticles were prepared through the borohydride-mediated reduction of $HAuCl_4$. 5-(1,2-Dithiolan-3-yl)-N-(prop-2-yn-1-yl)pentanamide (TP) was added into the as-prepared AuNPs solution as the capping agent. The azide part of azidoacetic acid and the acetylene part of TP were combined to form a triazole structure under the click reaction. The synthesized TTA–AuNPs can be used for further studies (Scheme 1). HR-TEM images revealed that the size of TTA–AuNPs ranged from 1 nm to 9 nm, with an average size of 4.9 nm (Fig. 1). The cycloaddition products from the click reaction were verified by infrared spectroscopy (Fig. 2). For TP–AuNPs (Fig. 2a), the peaks at $2934\ cm^{-1}$ and $3227\ cm^{-1}$ represents CH_2–S and N–H stretches, respectively, while the peak at $2116\ cm^{-1}$ represents C≡C stretches, indicating that TP was modified onto the surface of AuNPs. In Fig. 2b, the peak that was originally at $2116\ cm^{-1}$ (–C≡CH) disappeared, while a broad band between $2800\ cm^{-1}$ to $3500\ cm^{-1}$ (O–H) appeared, indicating that the click reaction proceeded on the surface of AuNPs.

3.2 Metal ion binding study

To evaluate the selectivity of TTA–AuNPs toward various metal ions, the absorption spectra of TTA–AuNPs were measured in the presence of 16 metal ions: Ag^+, Al^{3+}, Ca^{2+}, Cd^{2+}, Co^{2+}, Cr^{3+}, Cr^{6+}, Cu^{2+}, Fe^{2+}, Fe^{3+}, Hg^{2+}, Mg^{2+}, Mn^{2+}, Ni^{2+}, Pb^{2+}, and Zn^{2+}. In Fig. 3, only Pb^{2+} induced an obvious absorption change and color change from wine-red to purple, both indicating the aggregation of AuNPs. As a result of this aggregation, the absorbance at 519 nm decreased while the absorbance at 700 nm increased. Therefore, TTA–AuNPs shows excellent selectivity on Pb^{2+} over other metal ions. Pb^{2+} induced
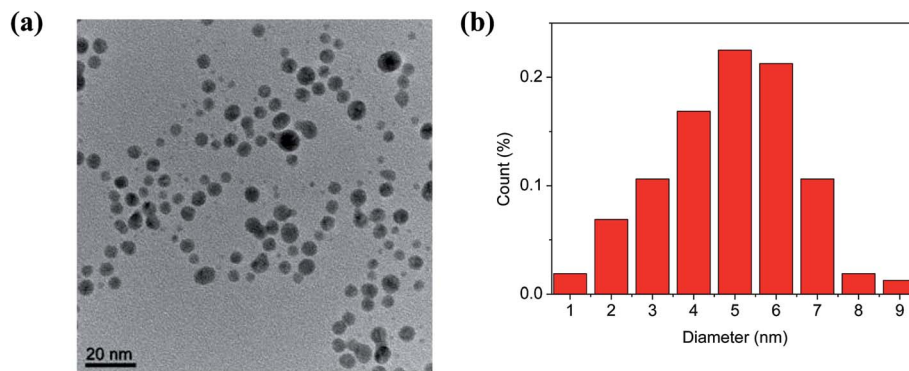
Fig. 1 (a) TEM image of TTA–AuNPs. The scale bar is 20 nm. (b) The size distribution of TTA–AuNPs.

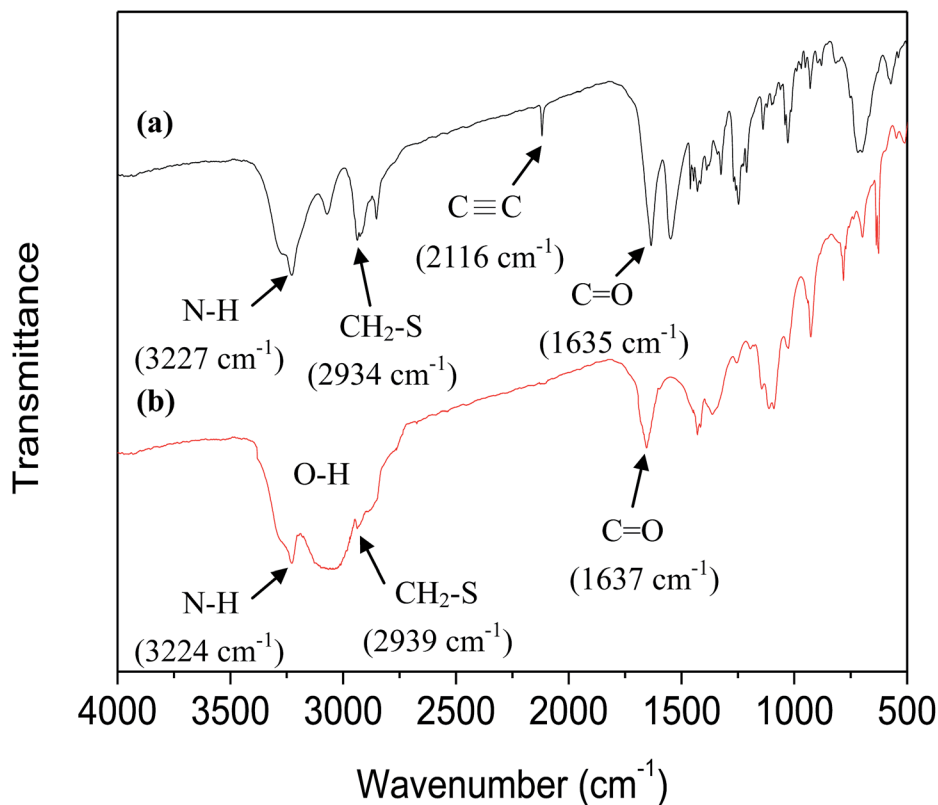Fig. 2 FT-IR spectra of (a) TP–AuNPs and (b) TTA–AuNPs.

aggregation of TTA–AuNPs is evident in the HR-TEM images (Fig. 4). Pb^{2+} has effectively functioned as a bridge between particles, triggering the aggregation of TTA–AuNPs (Scheme 2). This bridging interaction between Pb^{2+} and TTA was conducted through the carboxyl group and triazole structure (present in TTA on the surface of TTA–AuNPs).

3.3 The influence of pH on Pb^{2+}-induced aggregation of TTA–AuNPs

To investigate the pH range in which TTA–AuNPs could effectively detect Pb^{2+}, a pH titration was carried out. Fig. 5 shows that the absorbance ratio (A_{700}/A_{519}) of TTA–AuNPs increased when pH values were less than 5. Protonation of carboxylate anions resulted in the aggregation of AuNPs *via* hydrogen binding under acidic conditions (pH < 5). In the pH range of 5 to 12, the absorbance ratio (A_{700}/A_{519}) was constant, indicating that TTA–AuNPs were stable in this pH range. After addition of Pb^{2+}, the absorbance ratio (A_{700}/A_{519}) increased significantly in the pH range of 5 to 10. At pH > 10, the absorbance ratio (A_{700}/A_{519}) decreased due to the formation of colloidal $Pb(OH)_2$. Thus, conditions at pH 5 to 10 are suitable for monitoring Pb^{2+} by means of absorption change.

The degree of aggregation of TTA–AuNPs depends on the concentration of Pb^{2+} ions. The absorption spectra changed with the addition of different concentrations of Pb^{2+} (Fig. 6).
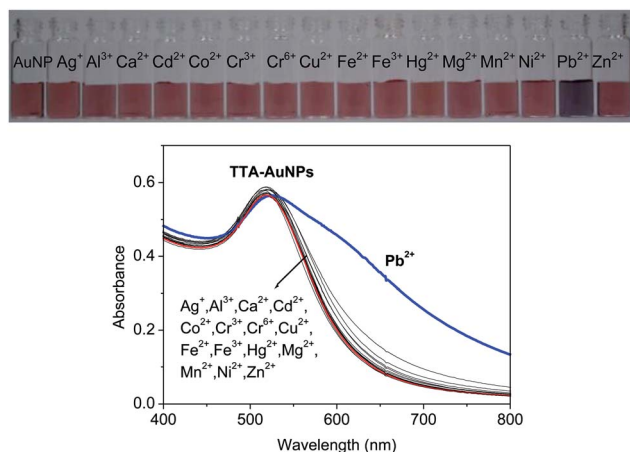
Fig. 3 Photographic images (top) and UV-vis spectra (bottom) of TTA–AuNPs in the presence of various metal ions (5 µM).
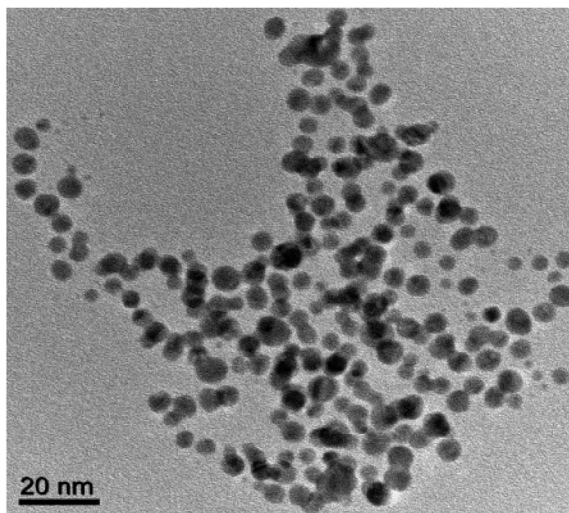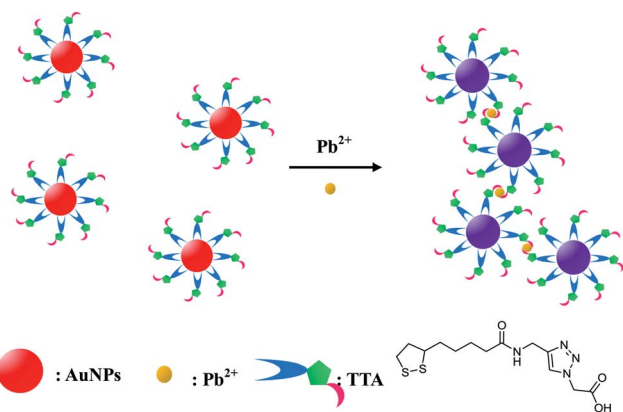

Fig. 4 TEM image of TTA–AuNPs in the presence of Pb^{2+} (5 µM).

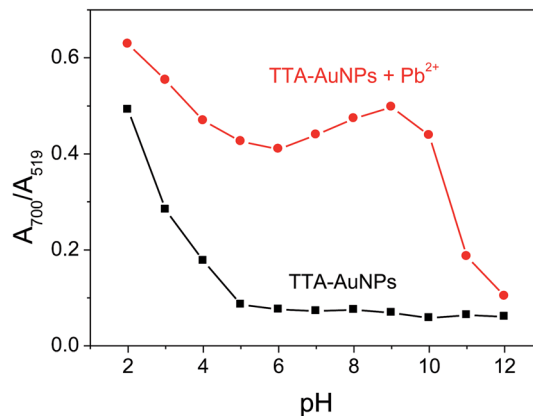**Scheme 2** Schematic depiction of Pb^{2+}-induced aggregation of TTA–AuNPs.

Fig. 5 Influence of pH on the absorbance ratio (A_{700}/A_{519}) of TTA–AuNPs in the absence (■) and presence (●) of Pb^{2+} (5 µM).
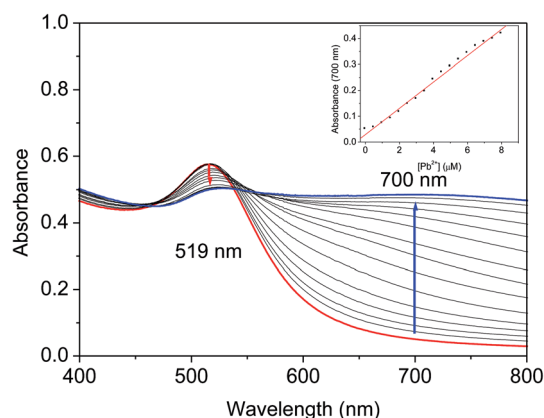

Fig. 6 Absorption spectral changes of TTA–AuNPs in the presence of different concentrations of Pb^{2+}. The inset shows the corresponding plot of the absorbance (A_{700}) versus Pb^{2+} concentration over the range of 0.5 µM to 8 µM.

The absorbance at 519 nm decreased while at 700 nm it increased with increasing Pb^{2+} concentration. A linear relationship was found in the plot of the absorbance at 700 nm (A_{700}) versus Pb^{2+} concentration over the range of 0.5 µM to 8 µM (inset plot of Fig. 6). The limit of detection for Pb^{2+} was found to be 16.7 nM.

Aggregated TTA–AuNPs can be redispersed by removing Pb^{2+} ions with EDTA; this was confirmed by the consequent SPR absorption shift from 700 nm to 519 nm (Fig. 7). After removing the solution using a centrifuge and suspending it with an aqueous media, the dispersed TTA–AuNPs can be reused to detect Pb^{2+}. Through this technique, the TTA–AuNPs system can be used repeatedly for the detection of Pb^{2+}.

3.4 Interference study

In order to study the influence of other metal ions on Pb^{2+} binding to TTA–AuNPs, competitive experiments were carried out in the presence of Pb^{2+} with Ag^+, Al^{3+}, Ca^{2+}, Cd^{2+}, Co^{2+}, Cr^{3+}, Cr^{6+}, Cu^{2+}, Fe^{2+}, Fe^{3+}, Hg^{2+}, Mg^{2+}, Mn^{2+}, Ni^{2+}, and Zn^{2+} (Fig. 8).
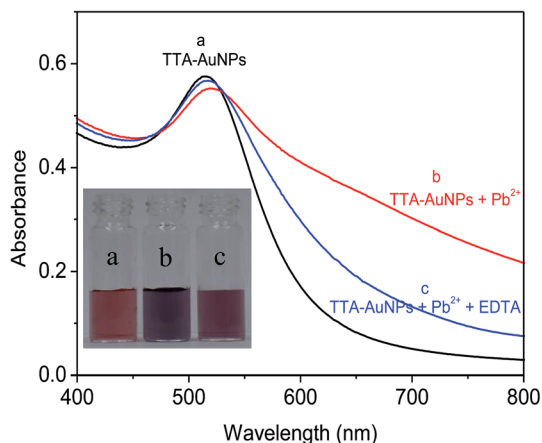
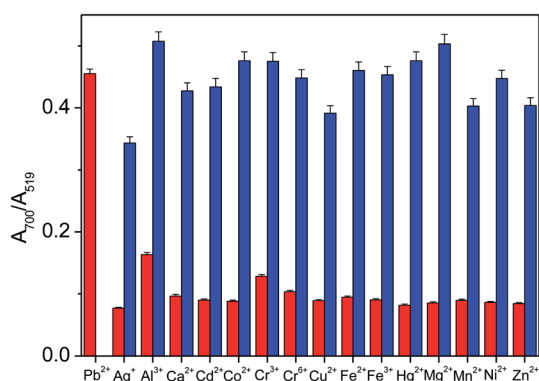**Fig. 7** Reversible binding of TTA–AuNPs with Pb^{2+} (5 μM) in the presence of EDTA (1 mM).

Fig. 8 Absorbance ratio (A_{700}/A_{519}) of TTA–AuNPs in the presence of metal ions. Red bars represent the addition of a single metal ion (5 μM); blue bars represent the mixture of Pb^{2+} (5 μM) with another metal ion (5 μM).

The absorbance changes caused by the mixture of Pb^{2+} with the other metal ions were similar to that caused by Pb^{2+} alone. This indicated that none of the other metal ions interfere in the binding of TTA–AuNPs with Pb^{2+}. This finding is consistent with the previous study suggesting that Pb^{2+} was the only metal ion that could bind to the TTA–AuNPs.

3.5 Analytical application in lake water

To confirm the practical application of TTA–AuNPs, a water sample from the lake located in NCTU, Hsinchu, Taiwan, was

Table 1 Results of Pb^{2+} detection in lake water samples

Sample	Added (μM)	Found^a (μM)	Recovery (%)	RSD (%)	ICP-MS (μM)
Lake water	2.5	2.47	98.8	1.6	2.34
	4.5	4.39	97.6	1.2	4.27
	7.5	7.65	102	1.5	7.48

^{a} $n = 3$.

collected and spiked with different amounts of Pb^{2+} standard solution. A calibration curve of TTA–AuNPs absorbance ratio (A_{700}/A_{519}) in the presence of different concentrations of Pb^{2+} was prepared (Fig. S2†). The analytical results are shown in Table 1. The recovery ranged from 97.6% to 102%, and RSD from about 1.2% to 1.6%. The results obtained with TTA–AuNPs are in good agreement with those obtained by ICP-MS. These results demonstrate that the designed probe is applicable for Pb^{2+} detection in lake water samples.

4.   Conclusion

In summary, new triazole-acetate functionalized gold nanoparticles have been developed for colorimetric sensing of Pb^{2+} ions. The functionalized sensor for colorimetric sensing of Pb^{2+} exhibited high selectivity in the presence of other interfering metal ions. This sensor offers a fast method for monitoring Pb^{2+} at a low cost and allows detection of concentrations as low as 16.7 nM. The optimal pH range for Pb^{2+} detection using TTA–AuNPs was determined to be 5 to 10. The sensor was applied to the analysis of Pb^{2+} in lake water with recovery ranging from 97.6% to 102%.

Acknowledgements

References

1 B. P. Lanphear, *Science*, 1998, **281**, 1617–1618.
2 H. Needleman, *Annu. Rev. Med.*, 2004, **55**, 209–222.
3 C. R. T. Tarley, F. N. Andrade, F. M. de Oliveira, M. Z. Corazza, L. F. Mendes de Azevedo and M. G. Segatelli, *Anal. Chim. Acta*, 2011, **703**, 145–151.
4 A. Michalska, M. Wojciechowski, B. Wagner, E. Bulska and K. Maksymiuk, *Anal. Chem.*, 2006, **78**, 5584–5589.
5 S. Tang, P. Tong, H. Li, J. Tang and L. Zhang, *Biosens. Bioelectron.*, 2013, **42**, 608–611.
6 F. Li, L. Yang, M. Chen, P. Li and B. Tang, *Analyst*, 2013, **138**, 461–466.
7 M.-C. Daniel and D. Astruc, *Chem. Rev.*, 2004, **104**, 293–346.
8 C. Burda, X. Chen, R. Narayanan and M. A. El-Sayed, *Chem. Rev.*, 2005, **105**, 1025–1102.
9 D. Liu, Z. Wang and X. Jiang, *Nanoscale*, 2011, **3**, 1421–1433.
10 J. W. Liu and Y. Lu, *J. Am. Chem. Soc.*, 2003, **125**, 6642–6643.
11 K. Yoosaf, B. I. Ipe, C. H. Suresh and K. G. Thomas, *J. Phys. Chem. C*, 2007, **111**, 12839–12847.
12 F. Chai, C. Wang, T. Wang, L. Li and Z. Su, *ACS Appl. Mater. Interfaces*, 2010, **2**, 1466–1470.
13 C. Wang, C. Huang, Y. Lin, W. Chen and H. Chang, *Anal. Chim. Acta*, 2012, **745**, 124–130.
14 C. H. Chung, J. H. Kim, J. Jung and B. H. Chung, *Biosens. Bioelectron.*, 2013, **41**, 827–832.
15 Y. Zhang, Y. Leng, L. Miao, J. Xin and A. Wu, *Dalton Trans.*, 2013, **42**, 5485–5490.

16 D. Su, X. Yang, Q. Xia, F. Chai, C. Wang and F. Qu, *RSC Adv.*, 2013, **3**, 24618–24624.

17 Y. Chen, I. Lee, Y. Sung and S. Wu, *Talanta*, 2013, **117**, 70–74.

18 P. Rajakumar, R. Anandhan, D. Manoj and J. Santhanalakshmi, *RSC Adv.*, 2014, **4**, 4413–4419.

19 S. Wei, P. Hsu, Y. Lee, Y. Lin and C. Huang, *ACS Appl. Mater. Interfaces*, 2012, **4**, 2652–2658.

20 J. Gu, Y. Lin, Y. Chia, H. Lin and S. Huang, *Microchim. Acta*, 2013, **180**, 801–806.

21 R. Rajendra and N. Ballav, *RSC Adv.*, 2013, **3**, 15622–15625.

22 D. Garin, F. Oukhatar, A. B. Mahon, A. C. Try, M. Dubois-Dauphin, F. M. Laferia, M. Demeunynck, M. M. Sallanon and S. Chierici, *Bioorg. Med. Chem. Lett.*, 2011, **21**, 2203–2206.

23 N. Brabez, R. M. Lynch, L. Xu, R. J. Gillies, G. Chassaing, S. Lavielle and V. J. Hruby, *J. Med. Chem.*, 2011, **54**, 7375–7384.

This journal is © The Royal Society of Chemistry 2014